MJFAS
Malaysian Journal of Fundamental and Applied Sciences

Saniman *et al.* | Malaysian Journal of Fundamental and Applied Sciences, Vol. 19 (2023) 970-979

RESEARCH ARTICLE

Probing the Electronic Properties of Cu and CuO Thin Films via XANES utilizing Powder XRD System

Siti Sarah Saniman, Muhammad Firdaus Omar*

Department of Physics, Faculty of Science, Universiti Teknologi Malaysia, 81310 UTM Johor Bahru, Johor, Malaysia

Abstract This research introduces an alternative approach on materials characterization by developing an in-house X-ray Absorption Spectroscopy (XAS) system utilizing powder X-ray Diffraction (XRD) machine. The performance of the in-house XAS system was investigated by analysing the position of Cu K-edge and the absorption spectrum shape within the X-ray Absorption Near Edge Structure (XANES) region. Copper (Cu) based samples were used to test the performance of the system where Cu and Copper Oxide (CuO) thin film deposited on polyimide tape and silicon wafer (100) prepared through the deposition process carried out using RF Magnetron Sputtering machine. Phase confirmation analysis were conducted by XRD and the deposited films' thickness were measured by Scanning Electron Microscope (SEM). The laboratory-based XAS measurement was carried out using Rigaku SmartLab X-ray Diffractometer configured for Bragg-Brentano (BB) measurement mode. Molybdenum (Mo) target was used to produce white X-rays by energizing it near 20 keV ±0.01 keV. XRD measurements on XRD and SEM analysis proves successful deposition of pure Cu and CuO thin films and the film thickness measured is 1.432 µm and 0.680 µm respectively. The conclusive findings of the laboratory-based XAS measurements indicate successful acquisition of XAS data with similar spectrum shape of experimental Cu and CuO XANES in comparison with theoretical data. Next, experimental XANES shows clear observation of Cu K-edge peaks for Cu thin film at 8.9737 keV, while Cu K-edge for CuO thin films is not observable. Lastly, there is also presence of significant XANES broadening and which then effect consequent peak shiftings.

Keywords: X-ray Absorption Spectroscopy (XAS), Copper, X-ray Diffractometer (XRD).

Introduction

X-ray Absorption Spectroscopy (XAS) is well-known for its ability to analyse crucial structural details of a targeted element making it a powerful characterizing tool. The study of the absorption spectrum usually categorized by X-ray Absorption Near Edge Structure (XANES) which is within 50–100 eV of absorption edge spectrum, that probes the coordination number and electronic state of targeted element. Meanwhile, Extended X-ray Absorption Fine Structure (EXAFS) that extends above 100 eV of absorption spectrum provides information on the local electronic structure of the targeted element. The principle of XAS is highly advantages in characterizing wide range of samples due to the interaction of source directly to the selected atom, without the requirement of specific atomic arrangement. To complement this powerful tool, the technique requires the high brilliance of X-ray source of significantly great photon flux together with monochromator element that can provide high resolving ability to selected energy bandwidth. Synchrotron sources have an exceptional ability to generate highly concentrated, monochromatic beams by the acceleration of electron beam near speed of light. Together with sophisticated and well-establish control systems and detection systems, synchrotron facilities have become the centre of revolutionized scientific research. Thus nowadays, the X-ray spectroscopy study which can also be known as core-level-spectroscopy are commonly conducted at synchrotron centres.

While XAS experiments conducted at these large facilities yields great data resolution and provide high tunability due to implementation of the undulators, the highly competitive environment as well as limited

***For correspondence:**
firdausomar@utm.my

Received: 21 August 2023
Accepted: 7 Nov. 2023

accessibility somehow complicates reseachers to opt this approach. Thus in the recent years, several efforts have been made to bring the know-how of the synchrotron back to the neighborhood laboratory; the emergence of modern laboratory-based XAS. Different kinds of approaches have been researched in order to develop a XAS system that can provide data quality which are on par with the synchrotron facilities. One of the approaches was by *Seidler et al.* utilizing X-ray tube for X-ray source generation, Johann crystal implementing Rowland-circle geometry as wavelength dispersive element, and silicon drift detector for X-ray detection with an energy resolution of the system being 1 eV for photon energies ~5 keV to ~10 keV [1]. Another research was conducted by *Nemeth et al.* which introduces an alternative approach to the wavelength dispersive section by utilizing cylindrical analyzer crystals in the von Hamos geometry [2]. Both systems have been tested where the data output reliability was proven [3], [4]. Despite many efforts, the lack of equipment and alternative approach to conduct XAS analysis drive researchers' interest to conduct more research to make almost 'synchrotron quality' analysis to be more available for wider user.

Copper (Cu) in its metallic state is a great electrical conductor but its conductivity changes with the presence of oxidation state, due to Ohmic-Schottky transition. Metallic Cu has been known for a long time in the electrical industries for its extensive application opportunities due to its great conducting abilities, e.g usage in printed circuit board (PCB) [5], and recently, in advance study of flexible circuit boards (FCB) [6]. Meanwhile ceramic Copper Oxides (Cu_XO_X), like tenorites (CuO) is widely used in the wide range of applications like p-type semiconductors [7], and recently have been gaining interest for its potential application in the recent development of thin film solar cells [8]. Researches on the properties of Cu-based materials requires on characterizations which are sensitive to oxidation states, such as XAS. Thus this paper introduces an alternative approach on probing the electronic properties of Cu and CuO thin films via XANES utilizing powder XRD system.

Materials and Methods

Sample Preparation

Cu and CuO thin films were prepared using solid source ion plating technology which is RF Magnetron Sputtering [9]. Such approach was attributed to its high sputter yield for wide range of materials like insulator, conductor, semiconductor, polymer, ionic and covalent compounds compared to dc magnetron sputtering [10] . The samples were deposited on three different materials which is polyimide tape, silicon (100) wafer and glass slide. Prior deposition process, cleaning process using solvent cleaning method were conducted for the purpose of eliminating oil residues and organic substance on the surface of substrates such that Si wafers and glass slides were cleaned using acetone (99.9%), then proceed with ethanol cleansing (95%) and lastly rinsed with distilled water. The wafer and glass substrates were then dried using nitrogen gas [11]. The cleaned Si wafer and glass substrate together with a fresh polyimide tape were then placed into deposition chamber stage to initiate deposition process.

RF Magnetron Sputtering (13.5Mhz) from Magna Value Sdn Bhd is utilized for the deposition process with target Cu (99.9%) at power rate of 200 W. Figure 1 shows the illustration of the RF magnetron sputtering chamber during deposition process. The chamber was evacuated until the base pressure reached below 10^{-5} Torr and then the precursor gas (Argon) and reactive gas (O_2) (during CuO deposition) was released into the chamber. The chamber pressure was increased so that the deposition pressure was kept below 10^{-3} Torr throughout the deposition process at room temperature with gas flow ratio ($Ar:O_2$) and also the deposition time as in Table 1.Noting that the deposition parameters were carried just to ensure the formation of Cu and CuO thin films as an element on investigating the in-house XAS system utilizing powder XRD machine capabilities.

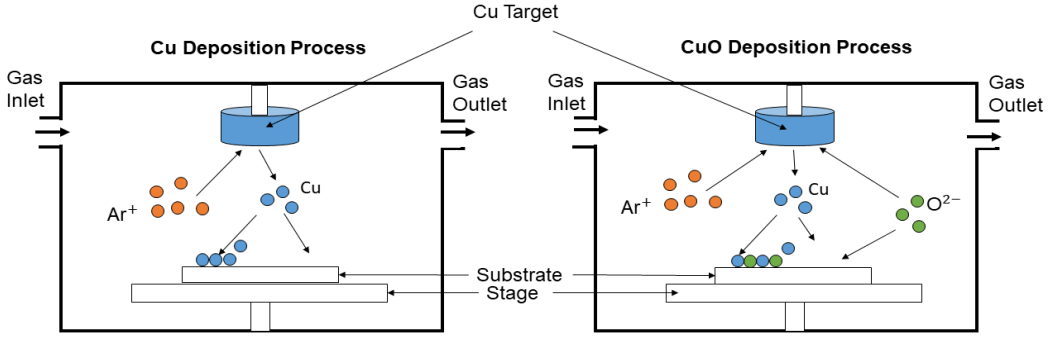

Figure 1. Deposition process of Cu and CuO

Table 1. Ar:O_2 ratio and deposition time for thin film samples

Samples	Ar:O_2	Deposition Time (hr)
Copper (Cu)	1:0	0.5
Copper Oxide (CuO)	5:1	1

Apparatus Setup

In this research work, the in-house XAS measurement is conducted using Rigaku SmartLab X-ray Diffratometer in the Bragg-Brentano (BB) measurement mode using 600 Watt cathode tube of Mo target as X-ray source with excitation energy near 20 keV to produce wider white X-rays or continuous X-rays energy range (Bremsstrahlung Effect) in comparison to the usual characteristic Cu K_α X-rays usually used in XRD analysis. Monochromator crystal A with a structure factor, $|F|$, of 181.26 is used to maximized the intensity of incident continuous X-rays to the sample. The system is equipped with D/teX Ultra 250 Silicon Strip Detector where the detector threshold or energy bandwith is optimized to increase peak-to-background ratio of XAS taken in transmission mode. Figure 2 shows a stainless steel slit that is made as sample holder with a hole of diameter, d=10 mm using the XRD Cu K_β filter measurements as reference.

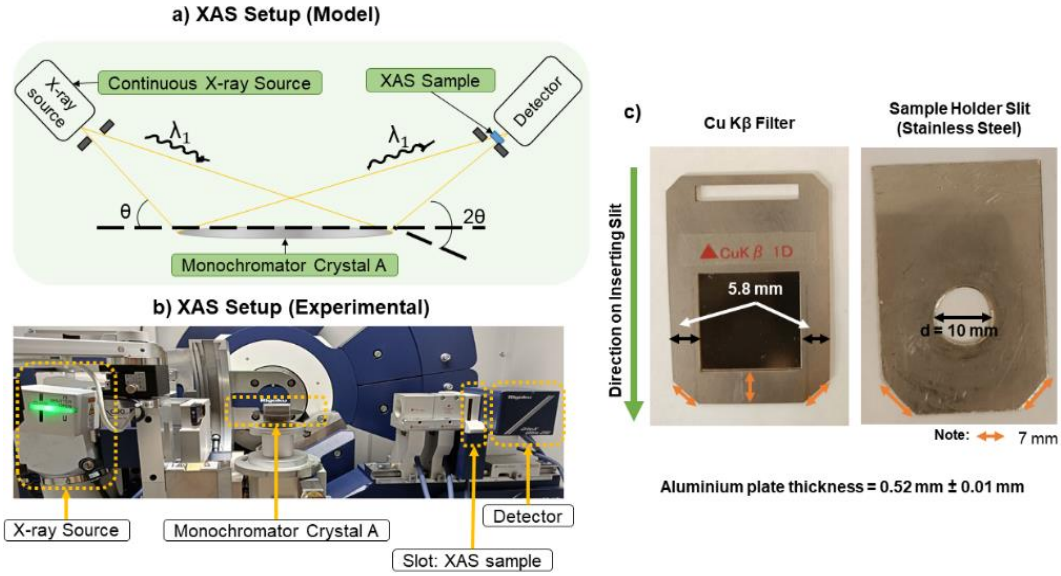

Figure 2. Model XAS Setup comparison to the experimental XAS setup

Characterization

The properties of Cu and CuO thin films were studied mainly using the in-house XAS measurement, while XRD and SEM were used as complementary analysis as means of confirmation on the materials' phase and thin film thickness respectively. Both in-house XAS measurement and XRD analysis utilised Rigaku SmartLab X-ray Diffractometer (SmartLab 2018 model), while SEM scannings were captured by SEM (JSM-5510LV), JEOL. In-house XAS measurement were performed on double layer of clean polyimide tape (I_o), as well as the deposited Cu and CuO thin films on polyimide tape substrate (I) at 8.95-9.04 keV for Cu and at 8.95-9.2 keV for CuO. Measurements were all collected at tube voltage of 20 kV and tube current of 30mA, and 10 scans were ran with an average of ~22 hours acquisition time for each sample. The averaging of the scans results in diminished noise providing a clearer observation of XANES oscillations. Further normalization and data processing were conducted using OriginPro Software [12].

Relationship of Beer-Lambert Law and Bragg's Law

XAS raw data which will be taken in θ/2θ measurement will be converted to linear absorption by sample thickness which is μt using Beer-Lambert Law:

$$I = I_o e^{-\mu t} \quad (1)$$

where I_o is the intensity of incident X-rays, I is the intensity of X-rays transmitted through the material, μ is the linear absorption and t is the thickness of the sample. The equation is then solved for μt plot:

$$I/I_o = e^{-\mu t} \quad (2)$$

$$\ln I/I_o = \ln e^{-\mu t} \quad (3)$$

$$\mu t = -\ln I/I_o \quad (4)$$

Then, since the absorption data was measured in the BB mode of θ/2θ measurement, a conversion of 2θ range to energy spectrum is conducted by applying the Bragg's Law:

$$2d \sin\theta = \lambda \quad (5)$$

where d is interatomic distance, θ is incident angle, and λ is the wavelength of incident X-ray. We know that the diffracted angle 2θ is twice the angle of incident X-ray thus the value of θ can be obtain by dividing the 2θ value by 2. Another related equation is the equation of photon energy:

$$E = hv = \frac{hc}{\lambda} \quad (6)$$

where h, is the Planck's constant and c is the speed of light and λ is the wavelength of photon (X-ray). The relationship of the Bragg's law and photon energy produces an equation for 2θ conversion to energy by combining equation 5 and 6, which will be:

$$E = \frac{hc}{2d \sin\theta} \quad (7)$$

Results and Discussion

Phase Confirmation and Film Thickness

Figure 3 shows XRD results of Cu thin film on polyimide tape shows the presence of polycrystalline face-centered cubic (fcc) Cu planes of (111), (200), and (220) at 2θ of 43.3˚, 50.46˚and 74.06˚, which agrees to the standard pattern for pure fcc Cu (DB card number : 7101264 : COD), RRUFF ID: R061078 and previous studies [13, 14, 15]. No impurity peaks of CuO and Cuprite (Cu_2O) were observed as the deposited Cu layer was immediately covered by another polyimide tape to avoid oxidation of sample. Meanwhile, the XRD analysis of CuO thin film shows the presence of polycrystalline monoclinic CuO planes of (110), (222), (-131), (20-2), and (-113) at 2θ of 32.17˚, 34.98˚, 38.30˚ and 65.61˚ which agrees with to the standard pattern for pure monoclinic CuO (DB card number : 9015841 : COD), RRUFF ID: R120076 and previous studies [16, 17, 18]. No peaks of Cu shows that during the deposition process, all Cu atoms and Oxygen (O_2) atoms have completely reacted before deposited on top of polyimide substrate. Peaks broadening and shifting could be observed from the XRD results from the lattice defects and atom dislocations [19]. Figure 4 shows SEM analysis taken using 5 kV Secondary Electron Image (SEI) under 10K magnification shows film thickness of Cu is around 1.432 µm, while for CuO taken using 3kV SEI under 20K magnification shows film thickness of 0.680 µm,

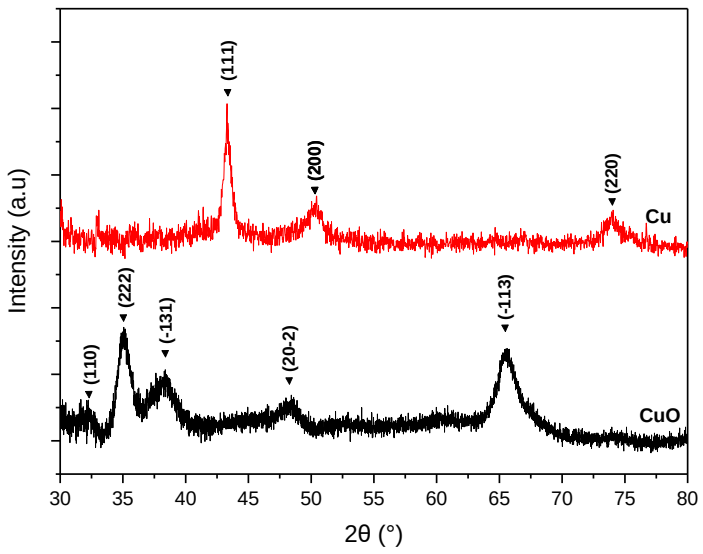

Figure 3. XRD results of deposited Cu and CuO thin films on polyimide tape substrates

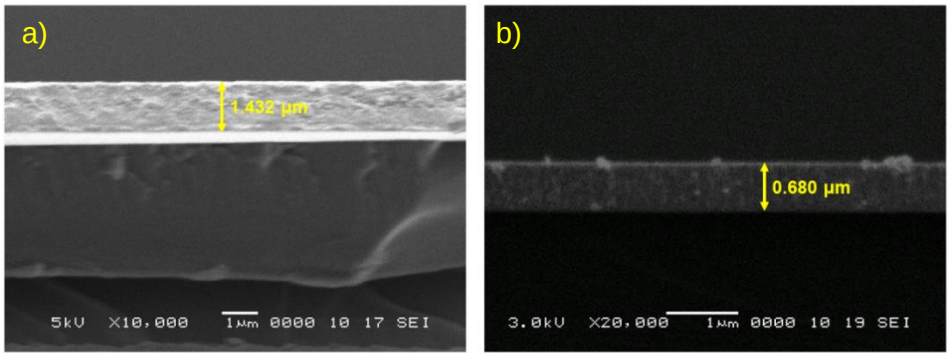

Figure 4. SEM results on the film thickness of a) Cu and b) CuO

In-house XAS Measurement

The in-house XAS measurements was taken in the BB mode using θ/2θ measurement. 10 Raw scans of Io_{Cu}, the intensity of X-rays incident to sample (Cu and CuO) and I, the intensity of X-rays absorbed by the X-rays were taken and then averaged to minimise background noise. Figure 5 shows a representation of the averaged scans taken for Cu and CuO where low X-rays intensity starts from 39.0˚ until 40.2˚. Past 40.2˚, the X-rays intensity suddenly went to a sharp rise of X-rays intensity, indicating an absorption jump at higher angle.

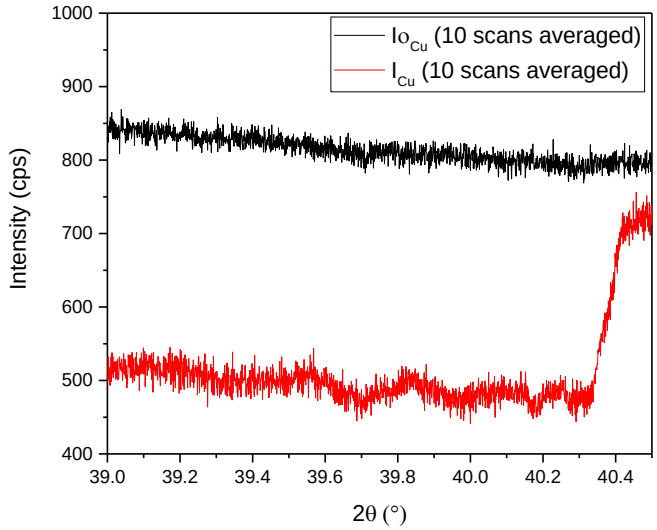

Figure 5. Averaged 10 scans of, the intensity of X-rays incident to sample (Io_{Cu}) and the intensity of X-rays absorbed by the X-rays (I_{Cu}) under θ/2θ measurement

The raw scans were then converted using the Beer-Lambert Law equation (Equation 1-4) for µt plot (Figure 6 a)). From the figure, the absorption of copper seems to drop over increasing 2θ range. According to the relationship of Bragg's law and the photon energy (Equation 7), where:

$$E \propto \frac{1}{\sin\theta} \tag{8}$$

which within the wide continuous X-ray source, high X-ray energy (shorter wavelengths) were dispersed by the monochromator crystal planes at lower angles, and with increasing θ/2θ measurement along the scanninig range, lower X-rays energy were diffracted. Thus, Cu K-edge absorption peak occurred at higher angle of lower energy (Theoritical Cu K-edge: ~8.979 keV). Furthermore, although the Figure 6 a) was able to better represent Cu absorption spectra than Figure 5, further conversion of 2θ range to energy range need to be done to identify the energy at which the absorption peak (K-edge) of Cu occurred. This can be carried out using the relation of Bragg's law and photon energy equation (Equation 7) with additional corrections from the system offset. Figure 6 b) shows the final product of XAS absorption spectrum with signal to noise ratio (SNR) of 1.47 calculated by the square root method:

$$\frac{S}{N} = \frac{S_{peak} - S_{noise}}{\sqrt{S_{noise}}} = \frac{(0.58 - 0.05) - (0.09)}{\sqrt{0.09}} = 1.47 \quad (9)$$

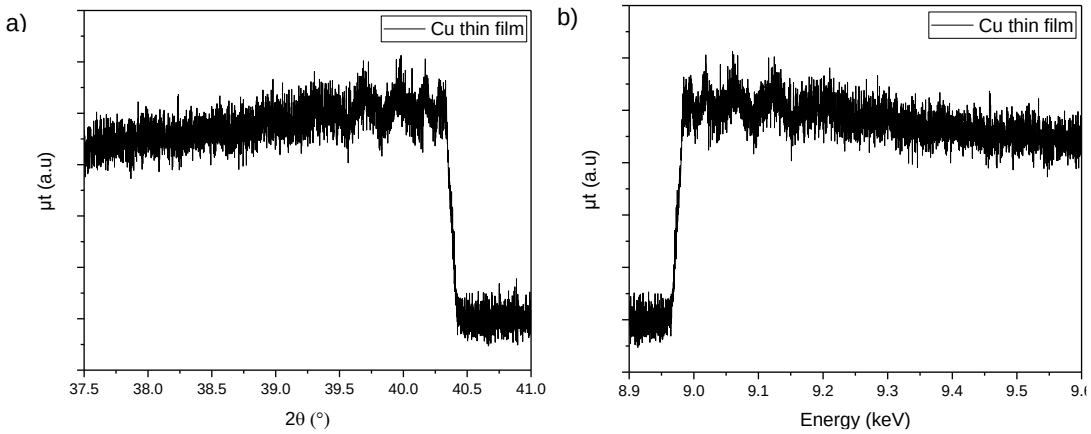

Figure 6. a) μt plot of Cu absorption over 2θ range, b) XAS absorption spectrum of Cu (μt plot of Cu absorption over energy range)

Figure 7 shows Cu element absorption spectrum within XANES region of experimental and theoretical absorption spectrum where further data processing of the experimental absorption spectrum were carried out by FFT bandpass filter with cut off frequency of 0~120 Hz and are normalized together theoretical data from Materials Project database. To compare the spectrum shape, an offset on the energy range of the theoretical data was performed to align the Cu K-edge. Note that the detector used in this research is D/teX Ultra 250 silicon strip detector where the distance between each strips is 75 μm (pixel width), the receiving slip opening is set 0.0225 mm throughout the measurement, and the distance from the monochromator to the detector is 300 mm. The broad structure of the experimental XANES is the result of the low energy resolution dispersion per pixel width @ over receiving slit opening of 75 μm to 0.225 mm which is minimum ~3 eV and varies at higher θ/2θ scanning angle. However, previous studies showed that deconvolution analysis on the XANES region results in significant reduction in K-edge broadening [20]. Furthermore, it can be seen that the magnitude of normalized experimental Cu K-edge is significantly lower compared to the normalized theoretical Cu while magnitude of normalized experimental CuO is comparable to theoretical. This results signifies an occurrence of self-absorption by Cu atom of Cu thin film sample implying that the sample's thickness surpasses of which is ideal, whereas CuO shows near to ideal sample thickness [21].

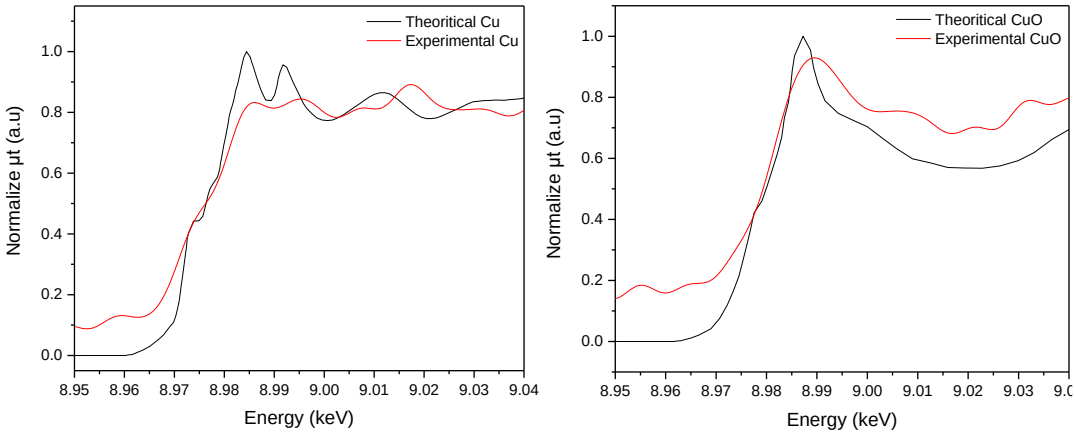

Figure 7. Comparison of theoretical and experimental Cu K-edge absorption of a) Cu and b) CuO

Figure 8 a) and b) show Cu K-edge XANES absorption spectrum which is sensitive to the local electronic state of probed Cu element, thus distinguishing the Cu species in the sample. Derivations for each spectrum was carried out for further clarification of the existing edges within the XANES region while

also identifies the presence of photon energy shiftings and broadenings. When Cu atom is in valency state of 0, Cu(0), also known as metallic form, its Cu K-edge (green dashed line) at 8.979 keV can be observed due to 1s to 4p electric dipole transition followed by small edge peak (purple dashed line) or a shoulder, then two maxima or crest (blue dashed line), meanwhile Cu(II) ions with valency of +2 shows weaker edge for the same electronic dipole transition, thus is usually identified by its singular crest position (pink dashed line) [22], [23].

From figure 8 a), the distinctive details of Cu(0) are all present within the theoretical Cu XANES, while the filtered experimental Cu XANES (red line: FFT bandpass filter of cut off frequency 0-120 Hz) Cu K-edge can be observed at 9.9737 keV and is lacking the details of shoulder edge past absorption edge (purple dashed line). Some peak shiftings can also be observed on the photon energy of the subsequent peak past the two maxima after edge peak (red dashed line) within the experimental Cu XANES with energy difference of 0.0218 keV compared theoretical Cu of 0.0198 keV, such that the shiftings can be caused by the broadenings of previous edges. On the other hand, as previously showed in Figure 7 where the magnitude of normalized experimental CuO XANES spectrum is comparable to theoretical due to achieving near to ideal thickness, Figure 8 b) shows that Cu K-edge (green dashed line) is not visible within experimental CuO XANES unlike theoretical CuO XANES, however the photon energy shifting is significantly lower where the photon energy difference from the first singular maxima (crest) to subsequent peak (red dashed line) with difference of 0.0629 keV for theoretical CuO XANES and 0.0646 keV for experimental CuO XANES. The lacking of the in-house XAS data quality is brought about by the low SNR and high energy resolution of the in-house XAS system. Figure 9 shows the Cu and CuO XANES spectra studied by *Wiktoria et al.* conducted by laboratory-based XAS system utilising X-ray tube – XOS X-BEAM Superflux PF with Mo anode (as X-ray source), the Cu K-edge of Cu and CuO samples can be observed at 8.980 keV and 8.983 keV respectively.

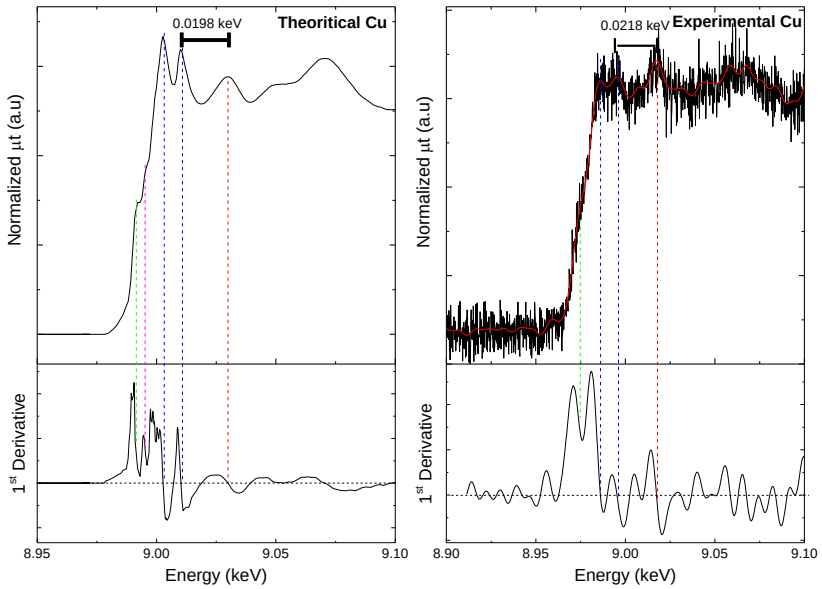

Figure 8 a). Cu XANES of Cu thin film samples for theoretical and experimental absorption spectrum and their derivatives

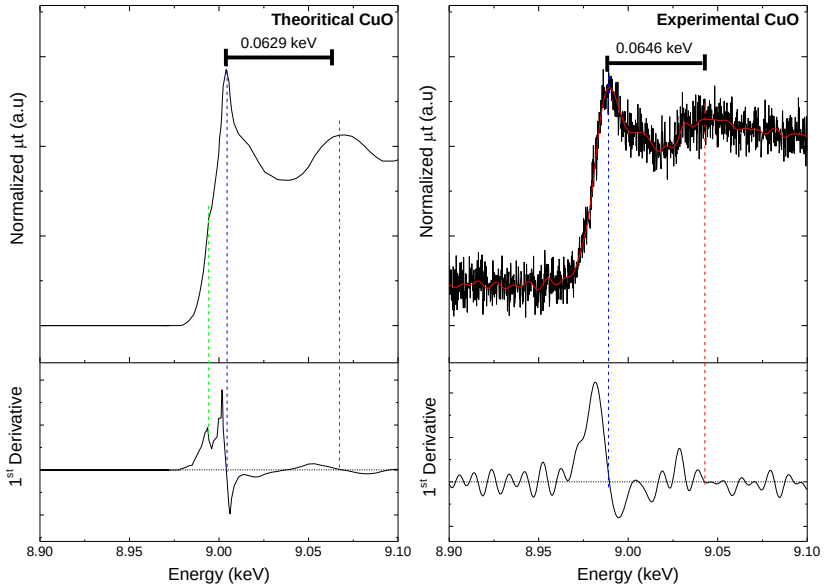

Figure 8 b). Cu XANES of CuO thin film samples for theoretical and experimental absorption spectrum and their derivatives

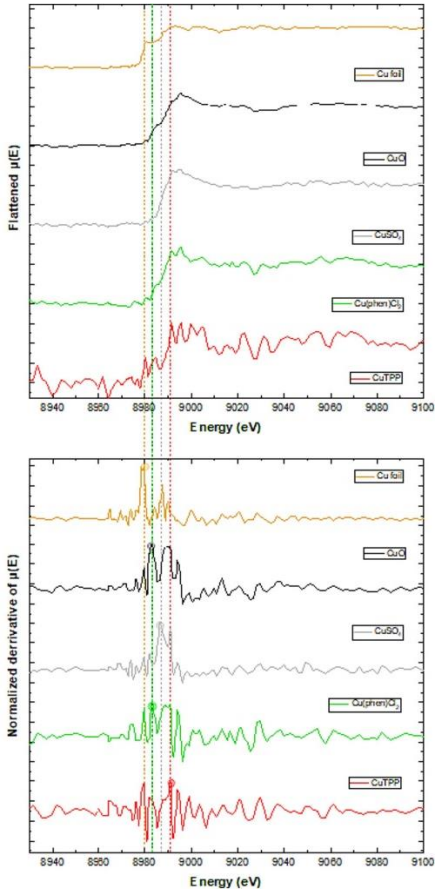

Figure 9. Cu and CuO XANES spectrum conducted by laboratory-based XAS system utilising X-ray tube – XOS X-BEAM Superflux PF with Mo anode (as X-ray source) [24]

Conclusions

In conclusion, the in-house XAS measurements utilising Rigaku SmartLab X-ray Diffractometer was able to measure the X-ray absorption of targeted element (Cu) eventhough there are presence of absorption peak broadenings and shiftings due to the low SNR and high energy resolution dispersion of the current system. The performance of the system can be further optimized by continuous research on the considerations and adjustments on the technical requirements especially for the enhancement of the SNR of in-house XAS measurements, such as incorporating a vacuum path to decrease X-rays scattering by air, or utilising crystal analyzers of higher-order reflection or higher structure factor. Regardless, the research is targeted to explore more alternative approaches on the XAS analysis, providing more options for routines laboratories analysis or to carry out preliminary investigations before conducting XAS analysis at the highly competitive but otherwise far advanced synchrotron facilities XAS beamlines.

Conflicts of Interest

The author(s) declare(s) that there is no conflict of interest regarding the publication of this paper.

Acknowledgment

Authors acknowledge the Ministry of Higher Education (MOHE) for funding under Fundamental Research Grant Scheme FRGS/1/2019/STG02/UTM/02/13 (Vot. No R.J130000.7854.5F243) and UTMFR Grant 21H25 for funding this project.

References

[1] G. T. Seidler *et al.* (2014). A laboratory-based hard x-ray monochromator for high-resolution x-ray emission spectroscopy and x-ray absorption near edge structure measurements. *Rev. Sci. Instrum.*, *85*, 11.
[2] Z. Németh, J. Szlachetko, É. G. Bajnóczi, and G. Vankó. (2016). Laboratory von Hámos X-ray spectroscopy for routine sample characterization. *Rev. Sci. Instrum.*, *87*, 10.
[3] D. Boglaienko *et al.* (2022). X-ray absorption spectroscopy of trivalent Eu, Gd, Tb, and Dy chlorides and oxychlorides. *J. Alloys Compd.*, *897*, 162629.
[4] R. Fanselow, M. Sobstel, W. Blachucki, and J. Szlachetko. (2022). *Performance of a laboratory von H mos type X‐ray spectrometer in X‐ray absorption.* John Wiley & Sons Ltd.
[5] S. Žák and R. Pippan. (2020). Cracks in thin Cu films on Si substrate – Plasticity influence. *Theor. Appl. Fract. Mech.*
[6] G. Girard, M. Martiny, and S. Mercier. (2020). Experimental characterization of rolled annealed copper film used in flexible printed circuit boards: Identification of the elastic-plastic and low-cycle fatigue behaviors. *Microelectron. Reliab.*
[7] S. Muthukrishnan, V. Subramaniam, T. Mahalingam, S. J. Helen, and P. Sumathi. (2017). Improved properties of spray pyrolysed CuO nanocrystalline thin films. *J. Mater. Sci. Mater. Electron.*
[8] S. Sinthamani, M. Ranjithkumar, S. K. Bharatan, S. Anitha, S. S, and S. M. (2022). Optical characterization of RF sputtered copper oxide for thin film solar cell application. *Mater. Today Proc.*
[9] F. Wang and J. Wu. (2023). Chapter 8 - Magnetron sputtering. *Modern Ion Plating Technology*.
[10] B. Ajit, A. Shampa, and T. T. (2022). Chapter 8 - Magnetron sputtering for development of nanostructured materials. *Design, Fabrication, and Characterization of Multifunctional Nanomaterials*.
[11] U. Irvine. (2010). Cleaning procedures for silicon wafers. *Fabrication*, 2-5.
[12] E. Seifert. (2014). OriginPro 9.1: Scientific data analysis and graphing software - Software review. *Journal of Chemical Information and Modeling*.
[13] RRUFF Project Database - Copper R061078." https://rruff.info/chem=Cu/display=default/R061078.
[14] A. Nasirian. (2012). Synthesis and characterization of {Cu} nanoparticles and studying of their catalytic properties. *Int. J. Nano Dimens.*
[15] J. Wang, H. Mi, W. Zhou, X. Yang, and Y. He. (2021). Preparation and tribological characteristics of graphene/triangular copper nanoplate composites as grease additive. *Ind. Lubr. Tribol.*
[16] RRUFF Project Database - Tenorite R120076." https://rruff.info/chem=Cu, O/display=default/R120076.
[17] S. Suresh, S. Karthikeyan, and K. Jayamoorthy. (2016). FTIR and multivariate analysis to study the effect of bulk and nano copper oxide on peanut plant leaves. *J. Sci. Adv. Mater. Devices*.
[18] M. Bin Mobarak, M. S. Hossain, F. Chowdhury, and S. Ahmed. (2022). Synthesis and characterization of CuO nanoparticles utilizing waste fish scale and exploitation of XRD peak profile analysis for approximating the structural parameters. *Arab. J. Chem.*
[19] T. Ungár. (2004). Microstructural parameters from X-ray diffraction peak broadening. *Scr. Mater.*
[20] P. D'Angelo, V. Migliorati, I. Persson, G. Mancini, and S. Della Longa. (2014). Quantitative analysis of deconvolved X-ray absorption near-edge structure spectra: A tool to push the limits of the X-ray absorption spectroscopy technique. *Inorg. Chem.*

[21] S. Calvin. (2013). Chapter 3.3 - Sample Characteristics for Transmission. *XAFS for Everyone*.
[22] W. Klysubun and Y. Thongkam. (2010). XAS study on copper red in ancient glass beads from Thailand. October 2017.
[23] S. Lin *et al.* (2020). Operando time-resolved X-ray absorption spectroscopy reveals the chemical nature enabling highly selective CO2 reduction.*Nat. Commun.*
[24] W. I. Stańczyk, J. Czapla-Masztafiak, W. Błachucki, and W. M. Kwiatek. (2023). Comparison between laboratory and synchrotron X-ray absorption spectroscopy setup examination of Cu(II) complexes with prospective anticancer properties. *Nucl. Instruments Methods Phys. Res. Sect. B Beam Interact. with Mater. Atoms*, *543*(August), 0-5.